Noise at the turn-on of a class-*B* laser

G. L. Lippi
Institut Non Linéaire de Nice, UMR 129 CNRS-UNSA, 1361 Route des Lucioles, F-06560 Valbonne, France

L. M. Hoffer and G. P. Puccioni
Istituto Nazionale di Ottica, Largo E. Fermi 6, I-50125 Firenze, Italy

(Received 5 May 1997)

We show through numerical simulations that different kinds of noise have different signatures in the statistical distribution of the intensity peak height as a function of delay time in the turn-on of class-*B* lasers. Simulations are carried out specifically for a CO_2 laser and are compared to the experimental results of H. Grassi *et al.* [Phys. Rev. A **50**, 805 (1994)]. Full qualitative agreement is found with the experiment. These results confirm that noise on the control parameter has a larger influence on the laser behavior than the intrinsic fluctuations. A physical interpretation of the role that the different physical noise sources play in the system is offered. [S1050-2947(97)08009-8]

PACS number(s): 42.55.−f, 42.60.Gd, 42.60.Mi

I. INTRODUCTION

The response to additive noise in a dynamical system governed by two variables that have quite different dynamical time scales has been analyzed in its general form in [1]. The authors have considered the transition of such a dynamical system away from an unstable fixed point towards a stable one and have investigated the influence that noise has on the system's trajectory in phase space. Two different ways of crossing the instability threshold have been examined: a sudden lowering of the relaxation constant for the faster of the two variables or the sudden increment of an external ''incoherent'' forcing.

It is a common occurrence in these dynamical systems that the representative point in phase space follows a trajectory that does not evolve directly from the unstable towards the stable fixed point, but rather spirals in towards the latter. The presence of noise affects the duration of the transition as well as the amplitude of the spiral itself. It was found [1] that if the transition is caused by a reduction of the relaxation constant for the faster variable, then the amplitude of the spiral decreases whenever the transition time increases. On the contrary, when the transition is caused by an increase in the incoherent forcing, the amplitude of the spiraling motion increases for longer transition times.

The generic situation described by the model in Ref. [1] is a good qualitative picture of the physics of crossing the lasing threshold in a class-*B* laser (e.g., solid state, semiconductor, and CO_2). Here the abrupt reduction of the relaxation constant of the fast variable corresponds to the reduction of the cavity losses (also called the ''loss switch'' or ''*Q* switch'' of the laser), while the increase in the incoherent forcing corresponds to increased pump strength (''pump switch''). Some measurements performed on lasers were presented in the same work [1], but a more complete experimental account appeared in [2], where a comparison between the two kinds of laser turn-on was performed on a CO_2 laser. Experimentally, the sensitivity of the system to noise translates into a dependence of the maximum of the field intensity overshoot on the delay time with which the laser turns on, measured with respect to the switch of the control parameter. In the two cases described above, increasing spiral amplitudes with increasing transit times are represented by maxima that align with a positive slope as a function of transit time (pump switch), while in the opposite case (loss switch) the maxima align with a negative slope.

In addition to confirming the predictions of [1], the experiment [2] showed that a more complex behavior in the sensitivity of the turn-on to noise exists: in the case of loss switching, the spiral amplitude is always smaller for increasing transit times, whereas in the case of pump switching, the amplitude could either increase or decrease for increasing transit times, depending on the relative amplitude of the noise sources. In the absence of a theoretical support for the observations, a heuristic interpretation for this occurrence was proposed [2].

In this paper, with the help of the numerical integration of a well-accepted model for a CO_2 laser [3], we investigate the effects of different noise sources on a laser subject to the two different kinds of turn-on. We show that one can obtain numerically the same kind of behavior observed in the experiment [2]. The advantage, offered by the numerical integration, of accessing both physical variables (population inversion and field intensity) and changing the strengths of the different noise sources allows us to give a clear interpretation of the role played by each noise source for each of the two turn-on mechanisms and to confirm the validity of the heuristic interpretation offered in [2].

Throughout most of this paper we concentrate on the discussion of the pump-switched laser, which presents experimentally the more puzzling behavior since the maxima of the peak intensity may line up, as a function of time delay, along a positive or a negative slope. Results obtained for the (simpler) loss-switched laser will be discussed only at the end of the paper for comparison and completeness. In Sec. II we briefly recall the features of the model employed. In Sec. III we discuss the details of the numerical realization of parameter switching and the application of the various kinds of noise, as well as the tests we performed on their reliability. Section IV is devoted to the discussion of the results ob-

 © 1997 The American Physical Society

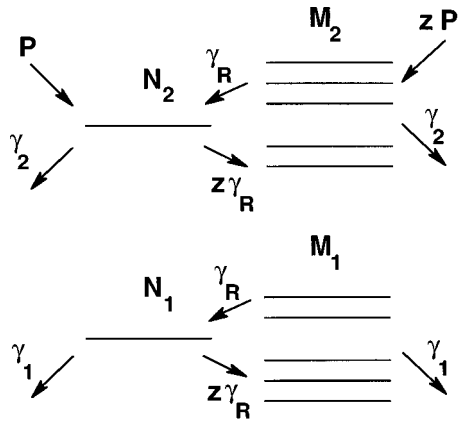

FIG. 1. Level diagram and definitions of variables and parameters used in the model. Nonlasing rotational sublevels are grouped in ''collective levels'' M_2 and M_1, belonging to different vibrational levels. The rotational sublevels N_2 and N_1, upper and lower lasing sublevels, respectively, couple to their rotational bands. Relaxation from the band to each level occurs at the rate γ_R, whereby the relaxation away from the lasing level is multiplied by the number of levels z present in the band, towards which the intraband relaxation may occur. Pumping P is assumed to be equal for all sublevels of the upper band and therefore to be z times higher for the grouped M_2 levels; relaxation away from the band, including the lasing sublevels, is assumed to take place at rates γ_2 and γ_1 for the upper and lower bands, respectively.

tained from the numerical integration and Sec. V to their interpretation. A brief discussion, in Sec. VI, on the quantitative comparison between numerical simulations and experimental results precedes the conclusions in Sec. VII. Some details about the form of the equations used in the integration as well as the values used for the constants for pump and loss switching are given in Appendixes A and B, respectively.

II. MODEL

We choose a model that describes the evolution of the laser with the help of rate equations. This choice does not affect the validity of the predictions since we want to interpret the experimental data obtained on resonance. However, there are several rate equation models available that describe the dynamics of a laser [4–6]. While capturing the basic physics of class-*B* lasers, these lower-dimensional models are not very well suited to describe the transient behavior and therefore we choose a model that fully includes in its description the particular characteristics of the CO_2 laser: the presence of the rotational manifolds coupled to the two lasing sublevels [3]. In fact, this latter model, which is an improved version of older ones [7,8], has been shown to provide a good description of the transient behavior of the CO_2 laser [3].

Its main features may be summarized as follows. Since laser action can take place only between two rotational sublevels of the vibrational manifolds [9], this model reduces the complex level structure to four effective levels (Fig. 1): two directly participating in the lasing action (N_2 and N_1) and two taking the place of all the remaining rotational sublevels in each vibrational manifold (M_2 and M_1). Such a treatment is justified by the fact that the rotational sublevels that are not coupled directly to the e.m. field interact very rapidly with the lasing sublevel that belongs to the same vibrational state and exchange population with it at a very high rate (much higher than the interband relaxation rate) [9]. At the same time, in a first approximation, they are indistinguishable in their interaction with the lasing level and therefore can be considered as a whole. Hence these levels can act as a reservoir of population for the upper lasing level and as a sink that depletes more rapidly the excess population of the lower level. In addition, in the CO_2 laser, the electrical discharge and the quasiresonant transition with the N_2 metastable state [9,10] do not pump selectively only the upper lasing level, but the whole vibrational band, therefore creating the reservoir of population inversion mentioned above.

With reference to Fig. 1, the laser model [3] can be written in the following form, where i is the field intensity, m_1 and m_2 are the normalized populations of the nonlasing collective sublevels, and n_1 and n_2 are the normalized populations of the two lasing sublevels:

$$\frac{di}{d\tau}=-\kappa[1-(n_2-n_1)]i, \tag{1a}$$

$$\frac{dn_1}{d\tau}=-(z\Gamma_R+\Gamma_1)n_1+\alpha(n_2-n_1)i+\Gamma_R m_1, \tag{1b}$$

$$\frac{dn_2}{d\tau}=-(z\Gamma_R+\Gamma_2)n_2-\alpha(n_2-n_1)i+\Gamma_R m_2+\Gamma_2 P', \tag{1c}$$

$$\frac{dm_1}{d\tau}=-(\Gamma_R+\Gamma_1)m_1+z\Gamma_R n_1, \tag{1d}$$

$$\frac{dm_2}{d\tau}=-(\Gamma_R+\Gamma_2)m_2+z\Gamma_R n_2+z\Gamma_2 P'. \tag{1e}$$

The variables that we employ here are a normalized version of those of Ref. [6], where

$$i=GI, \tag{2a}$$

$$m_1=\frac{G}{K}M_1, \tag{2b}$$

$$m_2=\frac{G}{K}M_2, \tag{2c}$$

$$n_1=\frac{G}{K}N_1, \tag{2d}$$

$$n_2=\frac{G}{K}N_2, \tag{2e}$$

$$P'=\frac{G}{K}P, \tag{2f}$$

$$\text{the overdot denotes } \frac{d}{d\tau}, \tag{2g}$$

and

$$\tau = \sqrt{\gamma_R K}\, t, \tag{3a}$$

$$\Gamma_R = \sqrt{\frac{\gamma_R}{K}}, \tag{3b}$$

$$\Gamma_1 = \frac{\gamma_1}{\sqrt{\gamma_R K}}, \tag{3c}$$

$$\Gamma_2 = \frac{\gamma_2}{\sqrt{\gamma_R K}}, \tag{3d}$$

$$\kappa = \sqrt{\frac{K}{\gamma_R}}. \tag{3e}$$

These normalizations have been chosen to obtain variables all $O(1)$ such that the numerical integration techniques may be as efficient and rapid as possible. The pump parameter P' is normalized to threshold, i.e., the laser crosses threshold when $P' = 1$. z is the number of interacting rotational modes. The steady states for the five variables, which we use as initial conditions (to be perturbed) for the integration, are given in Appendix A. The details of the normalizations used for loss switching are given in Appendix B.

III. NUMERICAL TECHNIQUES

We make the well-justified assumption [11] that the instantaneous noise amplitude just before the rapid commutation of the control parameter takes place has the most influence on the subsequent evolution of the trajectory in phase space from the unstable (laser below threshold) to the stable (laser above threshold) fixed point. Hence all the statistics are computed with no noise along the trajectory and are reduced to the ensemble of deterministic evolutions starting from random sets of initial conditions. This allows us to simplify considerably the calculations. At the same time, we see *a posteriori* that even in this approximation (noise *only* on the initial condition) a small amount of noise is sufficient to produce a sizable spread in the distribution of the peak amplitudes, thus highlighting the physical response of the system to the perturbation.

Operationally, the steady-state values for all variables are calculated as a function of the given input values for the parameters. Since we have adopted a stepwise commutation of the control parameter (pump or cavity losses) from its initial to its final value, we adopt the steady-state values as initial conditions and start the integration of the equations with the control parameter at a value corresponding to the laser above threshold. Noise is added to the variable(s) and/or parameter(s) chosen and in the amount decided by the operator. For example, noise in the initial value of the population is added directly to the steady state in the desired amount, while noise in the pump parameter is added to its value above threshold. Since the steady-state value for the macroscopic laser intensity is zero below threshold, and the computer could not obtain a growing intensity starting from this value, we have always set it equal to a very small constant (10^{-20} in normalized variables) to allow the trajectory to grow away from the unstable fixed point. We have also checked that the numerical value that we chose for this constant did not affect the results of the integration to any significant extent. When noise was added to the laser intensity, to simulate fluctuations in the spontaneous emission, we were always careful to choose noise levels much larger than this additive constant (at least four orders of magnitude larger).

The stochastic equations are integrated with a fourth-order Runge-Kutta method. To optimize for speed, the routine is streamlined and no error checking or automatic division of the integration step is included. Rather, we integrated repeatedly for the same parameters, reducing the time step for each run until the trajectory was clearly reproduced (implying that sufficient resolution was achieved). The time step used in the rest of the investigation was reduced from this value by another order of magnitude to ensure continued accuracy for all parameters. Noise has been introduced as δ correlated with high-quality random number generators having a very good flat frequency spectrum. Two different kinds of noise have been used in our investigations: white noise, obtained from a very long period random number generator [12], or Gaussian noise [13]. No difference in the slopes of the distribution of points have been found to result from the use of either kind of noise.

In order to check the stability of the algorithm in response to the abrupt variation of the control parameter, we tried three different shapes for the control parameter commutation: a step, a linear ramp, and a hyperbolic tangent, the latter two being fast with respect to the system's time constants, but containing many integration steps. In the first case, there is a large discontinuity in the control parameter over which the code has to integrate. For the linear ramp, the variation of the control parameter is continuous and is done with small enough steps so as not to perturb the numerical algorithm too much, but the derivatives are discontinuous at the two times when the ramp connects to the constant parts. The hyperbolic tangent time dependence of the control parameter offers the advantage of bypassing (almost entirely) both difficulties: the variation of the control parameter can be made to be very small and smooth over the switch and its time derivative is also nearly continuous everywhere (except for a small residual discontinuity coming from the fact that we do not integrate from $-\infty$ to $+\infty$, but this discontinuity can also be made to be very small). The advantage of the first method is its intrinsic speed, due to much simpler programing, while the last is the safest, but slowest.

The trajectories that we have obtained in the three cases are exactly superposable. Looking at the values of the maxima obtained in the three cases, one could see that they differed slightly only in the fourth digit past the decimal, thus showing that the integration algorithm is robust with respect to the sudden parameter switch. For this reason, all the integrations are done using the (simpler) step commutation.

The statistics are calculated always on small datasets (200 points). This choice is dictated by the desire to compare the numerical results to the experimental measurements of Ref. [2], where large datasets could not be obtained due to laser stability constraints. However, we have checked that the slopes do not change by mixing the results of several (up to

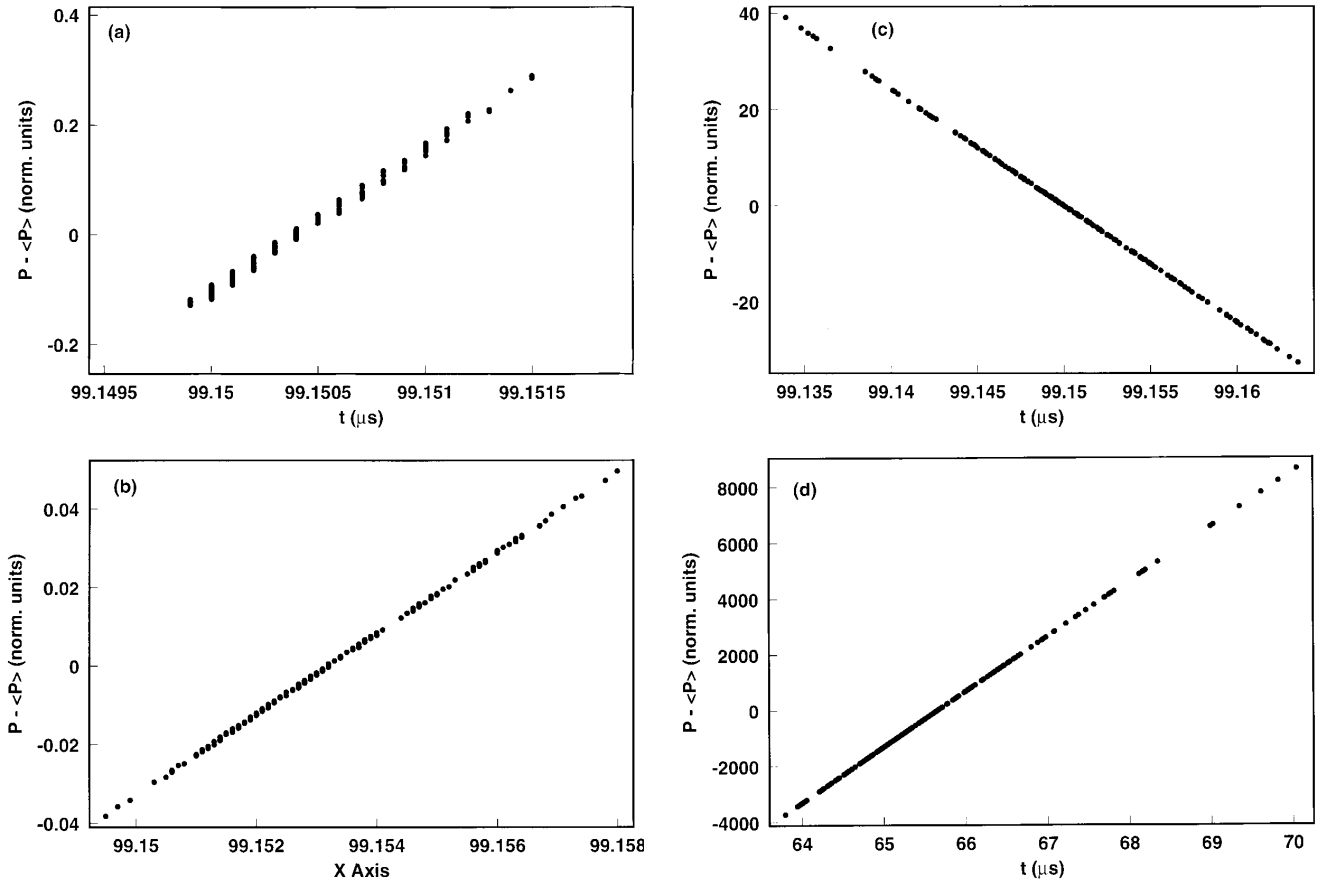

FIG. 2. Integration of the equations of the model for 200 initial conditions and noise on only one variable or parameter at a time: (a) noise on the population inversion (10^{-5} in normalized units), (b) noise on the cavity losses (10^{-5} in normalized units), (c) noise on the pump parameter (10^{-5} in normalized units), and (d) noise on the field intensity (10^{-5} in normalized units). The spacing between the points in (c), and partially also in (b) and (d), is due to a resolution limitation in the time output. Other integration parameters are defined, for this and the following figures, in Appendix A.

ten) different runs, as was also the case in the experiment, obtained from different seeds for the random number generator (the seeds are also randomly chosen).

The noise values are determined by the random number generator. For those runs where we have used the generator described in Ref. [12], which is normalized to 1, the output of the noise generator was multiplied by a noise amplitude coefficient to fix the absolute noise amplitude applied. Instead, when we used a random number generator with Gaussian amplitude distribution [13], the noise amplitude coefficient multiplied the characteristic amplitude width of the distribution. In both cases the noise amplitude has to be chosen to be sufficiently small if we want to obtain a linear distribution of points [14].

IV. NUMERICAL RESULTS

The numerical simulations confirm the interpretation of the different slopes observed in the experiment [2]. Noise ''internal'' to the system (e.g., acting on the population inversion, the cavity losses, or the electric field intensity) causes a distribution of points along a line with positive slope [Figs. 2(a), 2(b), and 2(d)] [15]. On the contrary, noise on the control parameter (the pump) gives a statistical distribution with a clear negative slope [Fig. 2(c)].

The amount of noise introduced on the field intensity variable is always much larger than the constant added to prevent the code from remaining on the zero intensity solution (about 10^{-25} of the steady-state field intensity above threshold). However, the applied noise is also rather small compared to the final steady-state value: about 10^{-8}–10^{-11} of the macroscopic steady state. Experimentally, this number is also quite small compared to typical noise values for a CO_2 laser. Nonetheless, the results that we obtain are still meaningful for the following two reasons. First we are interested in verifying the predictions of Ref. [1], where the linear approximation is taken, and therefore we are compelled to choose particularly small values of noise. Second, all models for CO_2 lasers, including the better ones (cf. Ref. [3]), are not capable of providing quantitatively correct predictions of the intensity of a realistic laser. Therefore, the results that we obtain can only be interpreted in relative terms and we can only look for the reproduction of the main physical features from the model. The actual values of the slopes or of the time intervals over which the points are spread cannot be considered to be correct in absolute terms [Fig. 2(d)]. Similarly, we have chosen the loss noise to be a small fraction of the cavity losses because of the very good mechanical and thermal stabilization in the experiment (cf. Ref. [2]).

We have imposed in Figs. 2(a) and 2(c) the same amount

of noise on population inversion and on the pump in order to take advantage of their common normalization. Because the scale of the two are comparable, it is useful to apply similar amounts of noise to compare the dynamical effects of the two noise sources. Figures 2(a) and 2(c) show that noise on the population inversion and on the pump affect the system in opposite ways. Having used the same noise strength on both sources allows us to make predictions about the relative sensitivity of the system to either one. For the example shown in the figure, both values amount to about 10^{-5} of their steady-state values, but we have performed simulations with noise levels up to 10^{-3} and beyond, values that are more consistent with experimental ones (cf. Ref. [2]). The results in this latter case are qualitatively the same, but are not presented here because they deviate from the linear approximation made in Ref. [1].

Figure 2 shows that ''intrinsic'' noise sources and ''control parameter'' noise (in the following referred to as ''control'' noise) act upon the system in different ways, giving rise to distributions of points that align according to opposite slopes. We will provide a physical interpretation of this fact in Sec. V. Let us now see what happens if we mix different kinds of sources, a condition that always occurs in the experiment. For the sake of clarity, we will limit ourselves to mixing only two noise sources at a time to show how their simultaneous presence influences the statistical distributions. We present in Fig. 3 the case where the two noise sources (a mix of intrinsic and control noise, on population and pump) have an opposite influence on the system, whereas in Fig. 4 we present the case where the two sources (a mix of two different sources of intrinsic noise, on population and cavity losses) have a similar influence on the system.

Figure 3 shows, as expected, that the sign of the slope characterizing the distribution of points is correlated to the relative strength and therefore predominance of either intrinsic [Fig. 3(a)] or control [Fig. 3(c)] noise, with an intermediate situation where neither dominates and no line can be defined [Fig. 3(b)]. We immediately remark that the relative amount of population to pump noise necessary to obtain slopes of either sign is quite different. While it is sufficient to have an amount of pump noise ten times larger than the population noise to obtain a clear negative slope, the population noise must be four orders of magnitude larger than the pump noise to make its characteristic slope predominate [16]. This result confirms the experimental observations [2] that a very high degree of stabilization of the control parameter is necessary to observe the effects of intrinsic noise in a CO_2 laser. Obviously, due to the large amount of spontaneous emission noise, this would not be the case in semiconductor lasers, where positive slopes in the distribution of the peak amplitude as a function of delay time were readily observed (cf. Refs. [17,18]).

Note that with pump noise in the numerical simulation, we reproduce several sources of noise present in the experiment. In addition to the ''true'' pump noise that comes from the fluctuations in the laser excitation current, two further, and related, experimental sources of noise are threshold fluctuations, coming from gas mixture fluctuations, and detuning fluctuations (cf. Ref. [2]). Both of them contribute to pump noise in the model, the first because the pump parameter is

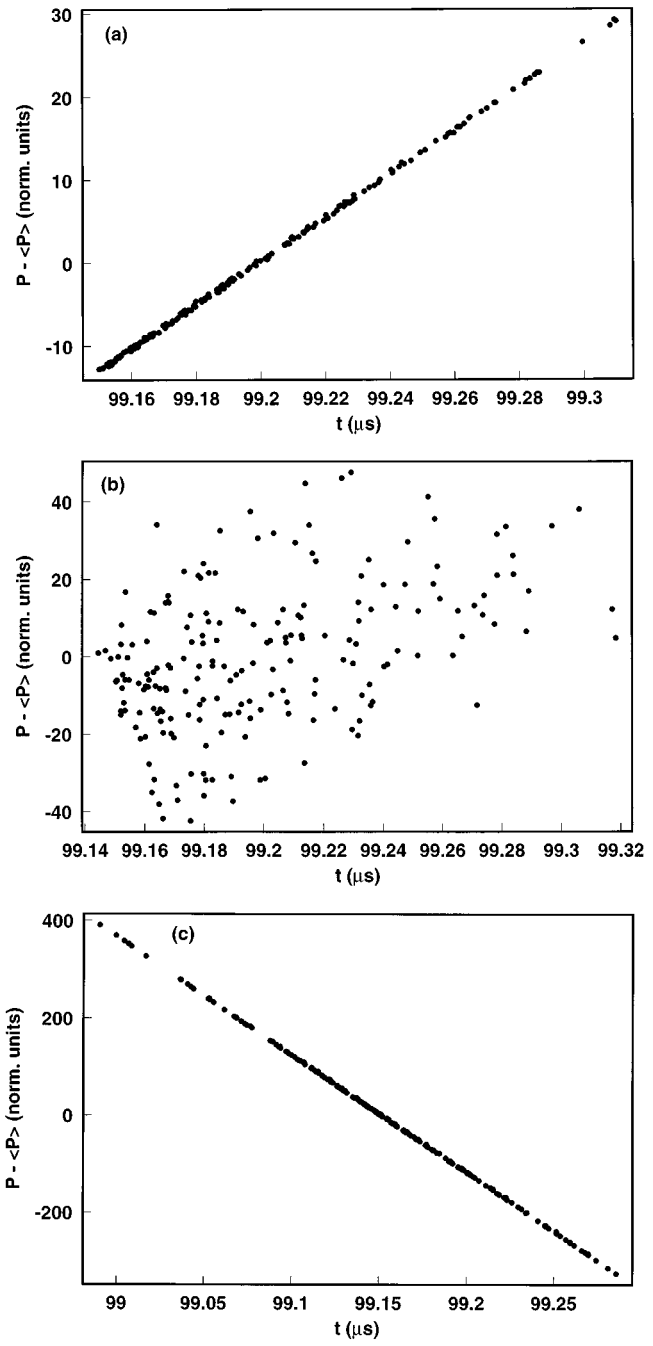

FIG. 3. Integration of the equations for two simultaneous kinds of noise. The ratio R_{pp} of population inversion noise to pump noise is (a) $R_{pp}=10^4$, (b) $R_{pp}=10^2$, and (c) $R_{pp}=0.1$. Notice that in (b) no slope can be defined, while the slope in (c) is about 10 times larger than in (a), thereby showing the greater effectiveness of control noise.

normalized to threshold, the second because the effective pump is defined as

$$P' = \frac{\mathbf{P}}{1+\delta^2}, \tag{4}$$

where δ is the detuning, in models that explicitly treat the field variable. Because of the absence of any reference in phase, there is no need to take detuning explicitly into account in this model.

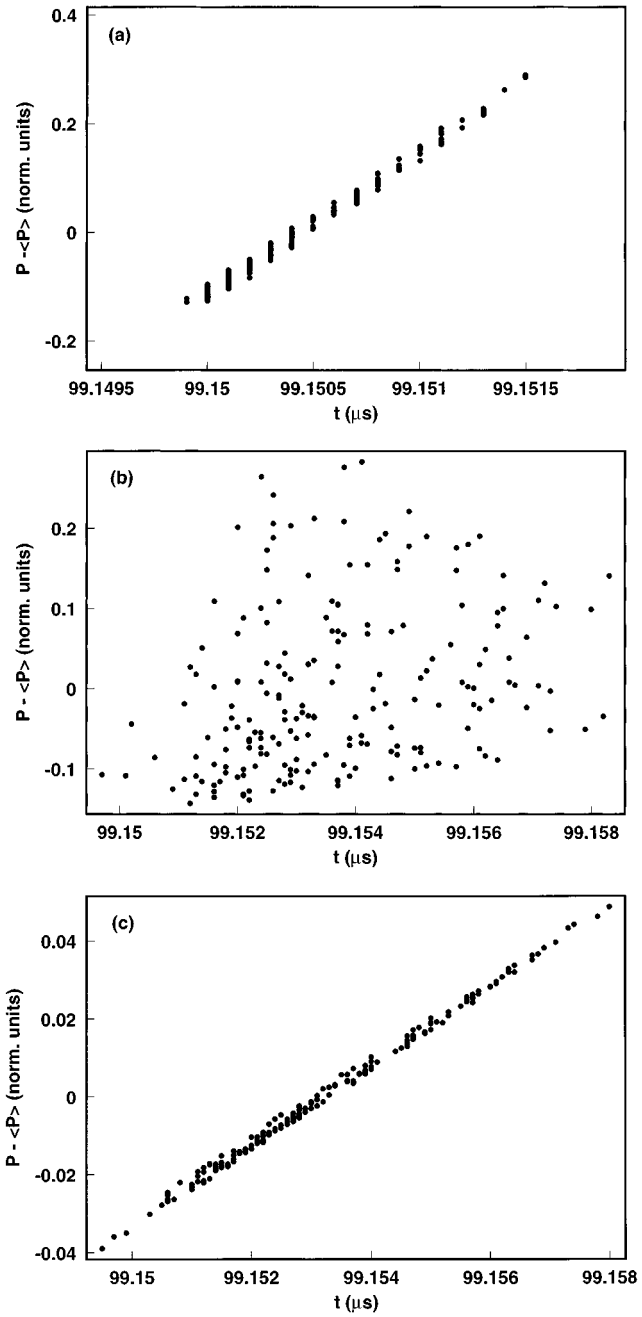

FIG. 4. Integration of the equations for two simultaneous kinds of noise. The ratio R_{pl} of noise on the population inversion to noise on the cavity losses is (a) $R_{pl}=100$, (b) $R_{pl}=1$, and (c) $R_{pl}=0.01$. Again, in (b) no slope can be defined, but the signs of the slopes in (a) and (c) are the same. Notice that the slope in (a) is two orders of magnitude larger than in (c); this difference in slope is the origin of the wedge-shaped point distribution in (b).

Fluctuations in the initial values of the population inversion are in our case indistinguishable from fluctuations in pump *below threshold*. In fact, since the population inversion is created by the pump, different initial values of pump give rise to different initial values of the population inversion. Thus, adding noise to the initial value of the pump does not affect the dynamics of the transient, but only creates a different initial population inversion, the latter being in equilibrium with the pump below threshold. On the other hand, noise on the final value of the pump plays an important role because it influences the dynamical evolution of the laser from the below-threshold to the above-threshold state.

Noise sources that affect the laser response in the same way change somewhat the value of the slopes without substantially affecting the shape of the distribution caused by a given kind of noise. The results of Fig. 3 explain very well those obtained from the experiment (cf. Ref. [2]). There (cf. Fig. 5), a change of slope was observed as a function of the residual amount of noise in the control parameter. As in the simulation, the transition from one situation to the other involves an intermediate state with a ''ball-shaped'' distribution of points through which no straight line can be reasonably fitted [Fig. 5(b)]. One further result of the simulations (not shown) is that for mixtures of noise values closer to the intermediate ball-shaped distribution, corresponding to situations where there is a non-negligible amount of noise of the nonpredominant kind, the ''thick'' distributions seen in the experiments are very well reproduced. While this effect could be intuited from the experimental results, its true origin can now be identified.

Finally, we show the consequences of mixing noise sources that affect the laser in a similar way. Figure 4 shows the results of the numerical simulation in the presence of noise added to the population and to the cavity losses. The distribution of points always maintains the same sign of the slope [Figs. 4(a) and 4(c)], but passes through a state where its ''linear'' shape is strongly altered [Fig. 4(b)]. This corresponds to the situation where the two noise sources have comparable ''strength.'' Since each of them has a positive slope, but with different magnitude, in the random sequence of pairs of noise coefficients for the same turn-on event, either of the two sources may predominate over the other, thus imposing its own characteristic slope. The global result is a point distribution that does not have a typical linear shape, but rather a more wedgelike distribution. On small datasets, and in particular in an experiment, the difference between this wedge-shaped form and the ball-shaped one from the previous case is completely masked. Hence the observation of a ball-shaped distribution of points may be due to either a mixture of noise sources with different effects on the laser or a mixture of noise sources with similar effects. The former situation can be unambiguously identified if, in addition, the sign of the slope changes when the relative strength of one of the noise sources is varied.

V. INTERPRETATION

A. Pump switching

The numerical investigation provides us now with a very powerful tool to test the interpretation of the experimental results proposed in Ref. [2]. Indeed, we can easily see why the two different kinds of noise should give rise to distributions with opposite slopes when the laser is turned on by switching the pump parameter. We first simulate the effect of noise on the population inversion between the two lasing states (n_2-n_1) by starting two noise-free simulations of the model with two different initial conditions (Fig. 6); the different initial conditions are intended to reproduce the effect of a noise fluctuation. The full time trace for the two intensities is shown in Fig. 6(b). The corresponding trace for the population inversion is shown in Fig. 6(a), where threshold is

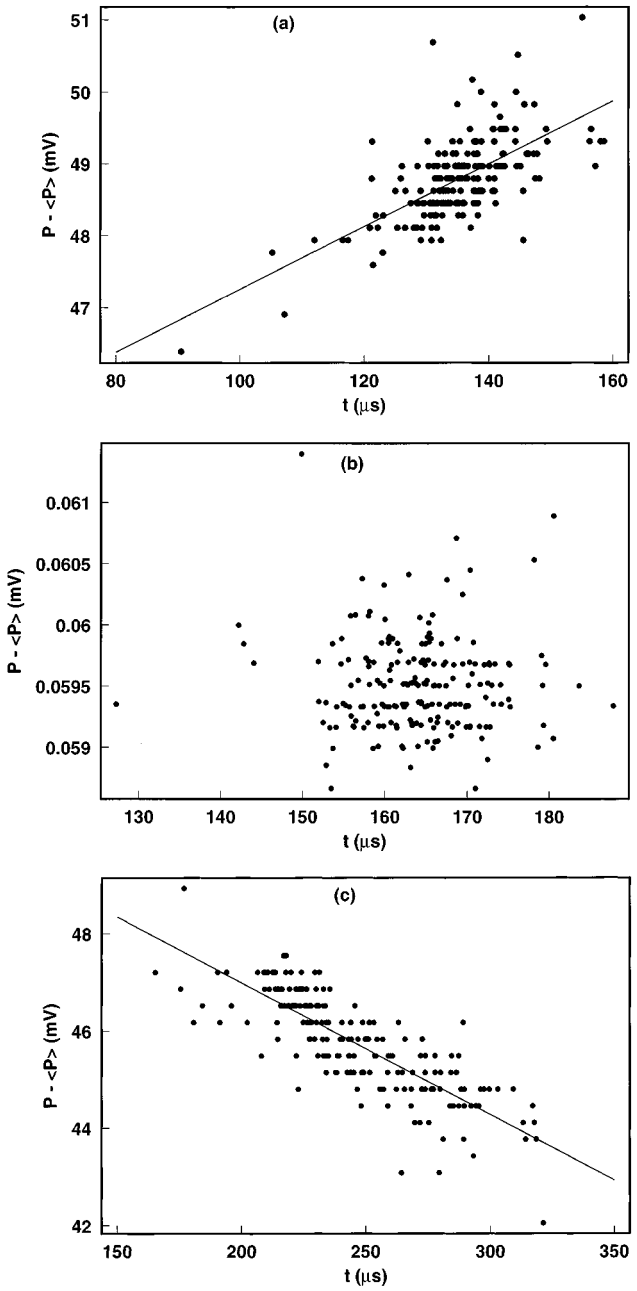

FIG. 5. Experimental distribution of peak intensity versus delay time from the experiment of Ref. [2]: (a) intrinsic noise is predominant; (b) intrinsic and ''control'' noise produce approximately equal effects: no slope can be defined in the distribution of points; (c) control noise is predominant. (a) and (c) are from Ref. [2] (Figs. 4 and 7, respectively). The longer delay times and lower peak amplitudes of (c) compared to (a) are due to the fact that the value of detuning, whose fluctuations are responsible for the control noise, is far off line center for the measurement of (c). The grouping of the experimental points along horizontal lines is due to the limit in resolution of the transient digitizer used in the measurements.

marked by a dash–double-dotted line and the final value of the pump parameter by a solid line. The pump step is applied at time equal to zero and the initial conditions are chosen to be very different for the purposes of illustration.

As we can see in the figure, the population inversion in the two cases starts from macroscopically different levels and grows in exponential-like form towards the upper final

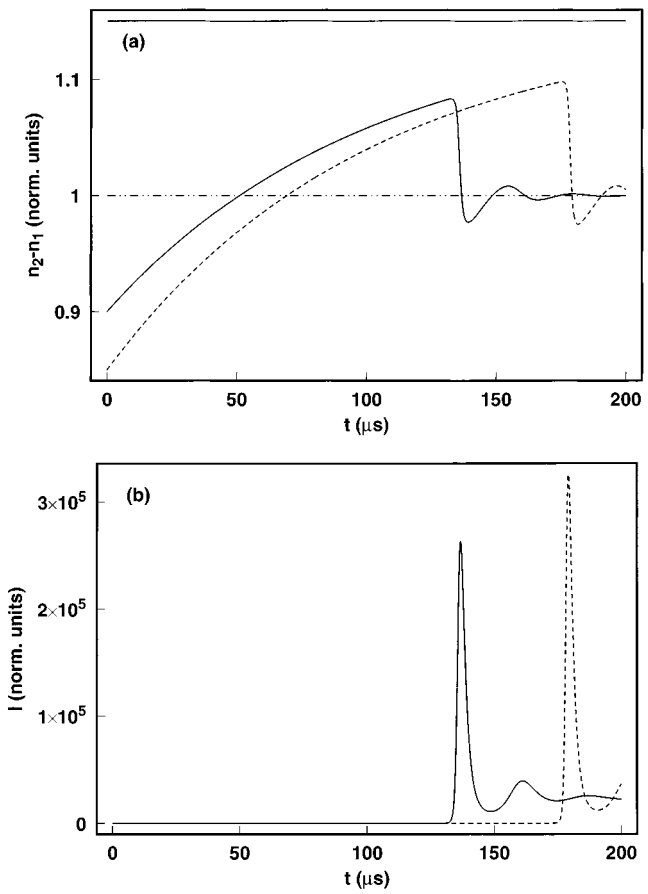

FIG. 6. Illustration of the effects of intrinsic noise on pump switching. The equations of the model are integrated with two different initial conditions to reproduce the effect of a fluctuation on the initial value of the population inversion. (a) Solid line, $n_2-n_1=0.9$; dashed line, $n_2-n_1=0.85$. The upper value of the pump, in both cases, is $P'=1.15$, as indicated by the solid horizontal line. The dash–double-dotted horizontal line represents the threshold. The characteristic exponential growth of the population inversion can be seen for times shorter than those necessary to attain threshold and an exponential-like growth is visible even beyond threshold, with an asymptotic tendency towards the upper value of the pump. The onset of the macroscopic field intensity (b) accompanies the abrupt drop of the population inversion below threshold, where it relaxes with underdamped oscillations. The spike in the laser intensity is due to the excess population value at the turn-on time.

value of the pump, which it should reach asymptotically in time if the laser intensity remains always zero. However, some time after the population has reached threshold the system bifurcates and the field's intensity grows away from the solution below threshold [cf. Fig. 6(b)].

During the growth time for the field intensity, i.e., after the time at which the population has crossed threshold, the population inversion continues to grow beyond the threshold level, since it is being ''used up'' to produce intensity at a negligible rate. However, when the field intensity becomes sufficiently large, a very strong spike takes place with a corresponding sharp fall in the population inversion below threshold. Since the lasing steady state corresponds to a value of the population inversion locked to threshold relaxation oscillations of the field intensity and of the population

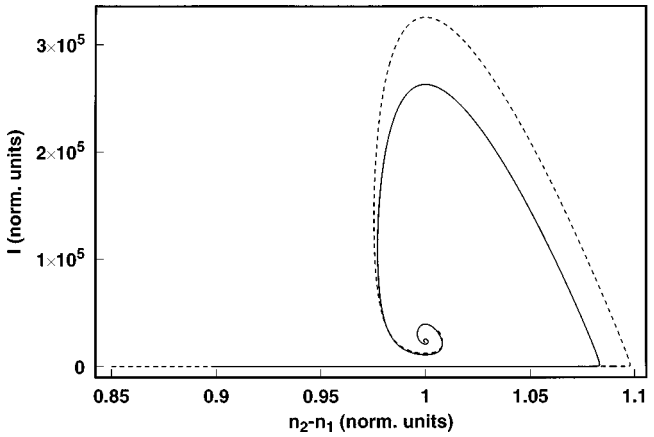

FIG. 7. Phase-space trajectories corresponding to the simulations of Fig. 6. The dashed line corresponds to the situation where the initial value of the population inversion is lower (cf. the dashed line in Fig. 6) and clearly shows that higher values of excess population inversion and higher intensity peaks are attained.

inversion (in phase opposition) ensue.

An important point to notice is that when the laser has started from a value that is farther away from threshold (dashed line), in the intervening time between the instant when the population inversion crosses the threshold and the intensity grows to macroscopic levels, there is a larger accumulation of excess population than for initial conditions nearer the threshold (solid line). This point is better illustrated in the phase space diagram (Fig. 7), where one clearly sees that the outer trajectory, corresponding to the larger peak amplitude in the intensity, is the one for which larger values of the excess population inversion are attained.

It is evident from Fig. 6 that this effect is to be attributed to the fact that the time at which the field intensity grows to macroscopic levels corresponds to higher values of the population inversion above the threshold value (dashed line). Hence, to longer delay times correspond higher levels of population inversion excess (due to noise fluctuations that lower the initial conditions of the population inversion) and therefore larger peak intensities. A distribution of points aligned with a positive slope in a graph of peak intensity versus delay time is therefore to be expected. A similar conclusion would be reached by repeating the same line of reasoning with noise on the intensity variable only (simulating spontaneous emission). In this case, to lower values of the initial intensity correspond longer buildup times for the pulse and hence larger values of excess population inversion, which give again larger pulses in correspondence to longer delay times.

There is a very similar effect for loss noise. If the losses are instantaneously increased due to a noise fluctuation, then the field intensity amplitude grows at a slower rate [as evident from Eq. (1a)]. Due to the slower growth of the intensity, the delay time is longer and the excess of population inversion that results is higher, thereby producing larger intensity peaks for longer delay times. Hence the points align again along a positive slope.

The effect of pump noise is shown in Fig. 8 by changing the final level of the pump macroscopically for the purposes of illustration. This example is sufficient to illustrate all cases we want to consider since, as already stated, threshold

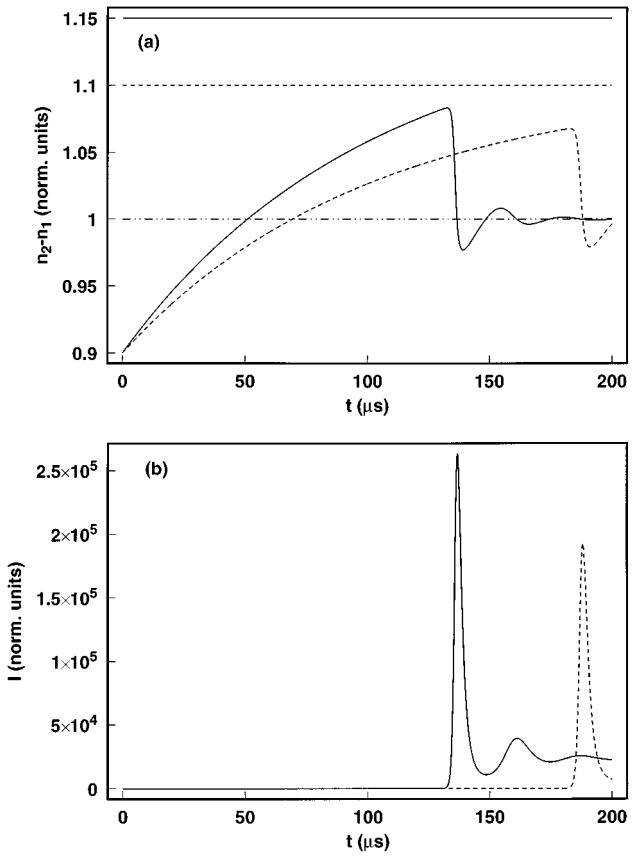

FIG. 8. Illustration of the effects of control noise on pump switching. The initial value of the population inversion is the same in both runs, while the effect of noise on the final pump value is simulated by choosing two different values for the pump above threshold. In (a) these two values are indicated as follows: $P' = 1.1$ (dashed horizontal line) and $P' = 1.15$ (solid horizontal line). The dash–double-dotted line marks the laser threshold. In (b) the longer delay time between the turn-on and the peak is due to the smaller final pump value. The smaller peak in the field intensity is due to a lower value of the excess population inversion attained during the delay after crossing threshold.

and detuning fluctuations can be directly connected to changes in the final pump. The two couples of time traces of Fig. 8 show two different situations starting from the same initial condition. For higher values of the final pump (solid horizontal line), the population inversion grows faster, reaches the threshold sooner, and crosses it with a local slope that is higher (solid time trace), attaining in the end a larger value of excess population. Just after the population crosses threshold, the intensity begins to grow, but at first its value depends mostly on its initial value (which is the same in both cases) and it is not large enough to affect the population growth in a macroscopic way. Since the growth rate of the intensity depends on the instantaneous value of the population inversion, for higher values of the final pump (solid line and corresponding solid time trace), it will reach macroscopic levels sooner. Thus a larger excess population will correspond to a shorter delay time, as well as larger peak intensity values, as seen in the figure. The slope that we then expect in the distribution of peak heights as a function of delay time is negative. This explains the behavior observed in the experiment and heuristically interpreted in [2].

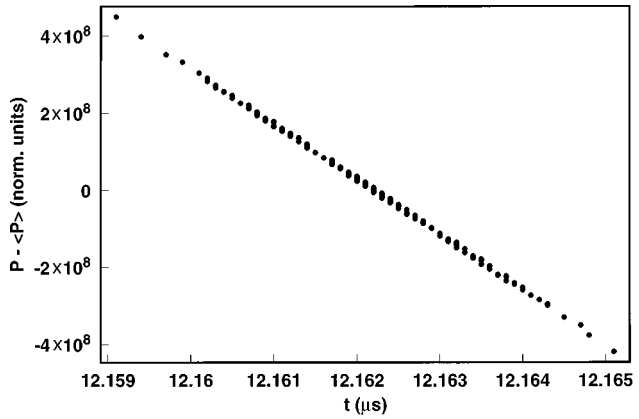

FIG. 9. Statistical distribution of intensity peaks as a function of delay time obtained from the integration of the model for loss switching with noise (10^{-5}) on the control parameter.

The numerical simulations that we have shown also illustrate one further point: the presence of a large deterministic delay time on which the stochastic component is superposed. This point was remarked upon in the experimental measurements (cf. Ref. [2] and Fig. 5) and is also visible in the simulations (Figs. 2–4). The deterministic component of the delay time comes from the slow buildup time of the population inversion, clearly shown in Figs. 6 and 8, while the superimposed stochastic spread comes from the spread of the delay times induced by noise (''simulated'' through different initial conditions in Figs. 3 and 4).

B. Loss switching

The numerical simulation of the model allows us also to elucidate a few points concerning loss switching. The equations used in these simulations are given and discussed in Appendix B.

The main feature of this kind of switching is the appearance of point distributions for the intensity peaks as a function of the delay time aligned along straight lines with negative slopes [1,2]. Figure 9 shows such a point distribution in the presence of noise on the cavity losses. The physical origin of the negative slope is the initial condition of the population inversion at turn-on. At the moment the losses are lowered, the population inversion is *immediately* above threshold. This implies (i) the immediate ability of the system to convert spontaneous emission into stimulated emission and (ii) a crucial sensitivity to the amount of feedback (i.e., the cavity losses).

In contrast to the case of pump switching, the population inversion remains in equilibrium with the pump at a constant value (cf. Fig. 10) for as long as the field intensity remains negligible. Since the laser finds itself suddenly in the inverted state, the factor controlling the statistical distribution of the peak amplitudes as a function of delay time is the growth rate of the intensity. A fluctuation (superposed on the loss switch) that further lowers the cavity losses implies a larger amount of excess population inversion available to the field intensity. The intensity in this case grows faster (since its derivative is proportional to the population excess) and also reaches a higher peak value. Hence we see in Fig. 10(a) that in the solid trace (which corresponds to a lower value of the losses), the population drops sooner to its final, lower

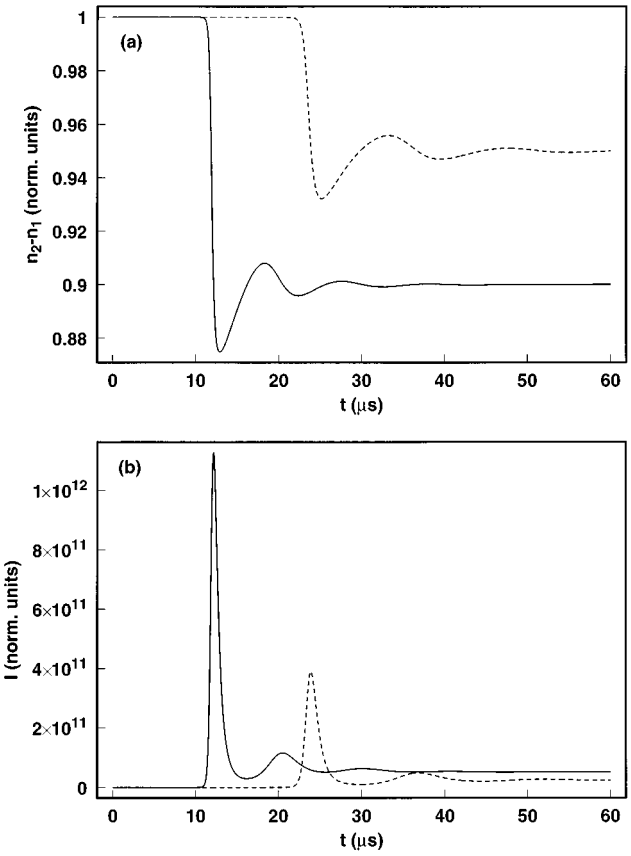

FIG. 10. Simulation of the effects of control noise on loss switching obtained by a deterministic integration of the model for two different final loss values. Notice that the population inversion (a) remains constant at its normalized initial value until the laser intensity (b) turns on. To a smaller final value of the losses (larger fluctuation) corresponds a larger slope of the intensity and hence also of the drop in population inversion as well as a larger excess of population inversion with respect to its final value.

value and there is an anticipation of the turn-on compared to the case with slightly higher losses (dashed line; the size of the loss fluctuations has been exaggerated for illustration purposes). Thus, to shorter time delays (due to a more efficient feedback) correspond higher values of the intensity peak [cf. Fig. 10(b)] and therefore the points distribute along a line with negative slope.

It is worth remarking that in pump switching, the excess population inversion available to the field intensity is only the amount built up during the delay time when intensity is still negligible. How much excess population accumulates depends on the growth rate of the population inversion, which is slow compared to that of the intensity. In the loss-switch case, on the other hand, the population inversion is already in saturation and the maximum possible amount of excess is ready for the switch to occur. Thus there is a much larger sensitivity to small fluctuations in the control parameter and a tendency towards larger peaks in the intensity. This explains why the slope of the line along which the points align is particularly large (in absolute value) for loss switching.

Due to the fact that the initial condition of the population inversion, in loss switching, is above threshold and is held constant by the pump until the field intensity becomes ''mac-

roscopic,'' the other noise sources we investigated do not have a sizable effect on the slope. Noise added on the intensity can reduce the delay time (the intensity grows to macroscopic values sooner if it starts from an initially higher value) and noise on the pump may vary somewhat the amplitude of the peak, but their effects are rather small. This, together with the extreme sensitivity of the system to noise on its control parameter, explains why the distribution of intensity peaks always has a negative slope.

Incidentally, this result also shows why the delay times in the loss-switching case are much shorter and no deterministic component can be observed (cf. Ref. [2]). As shown in Fig. 10, the population inversion is above threshold immediately after the switch and therefore the deterministic delay due to the (slow) growth of the population up to the threshold value is absent. Thus the delay comes exclusively from the stochastic growth of the field intensity out of noise. In our numerical simulation, Fig. 9, the initial condition for the field intensity is small compared to the amount of noise applied to the losses and therefore a ''deterministic'' noise component seems to still be present.

C. Summary

We can summarize the results of this section as follows. The application of intrinsic noise causes a point distribution in the intensity peaks that highlights the dynamical behavior of the population inversion after turn-on, whereas the control noise instead magnifies the intrinsic feature of the class-*B* system.

In the case of intrinsic noise, the population inversion starts below threshold and grows during the time delay in the case of pump switching (cf. Fig. 11, top left), with peaks placed along a line with a positive slope. In the case of loss switching, (cf. Fig. 11, top right, with noise on the initial field intensity value), the population inversion is constant and the peak intensity distribution is flat.

In the case of control noise, since class-*B* lasers are characterized by an overshoot of the intensity at turn-on (independent of the control parameter used for the commutation), an increment in the control parameter due to a fluctuation enhances the peak. When the laser is driven harder it turns on faster and the intensity peaks are placed along a line with negative slope (cf. Fig. 11, bottom). In the case of pump switching, depending on the relative amount of intrinsic versus control noise, it is possible to obtain either slope. For loss switching, a change in sign does not appear to exist and one can expect at most a reduction of the magnitude of the (negative) slope.

Although these illustrations are obtained starting from a model specific to CO_2 lasers, the basic features of these processes can be extended to all class-*B* lasers. In fact, on the basis of the general treatment on which slope predictions were based (cf. Ref. [1]), one could also claim that with appropriate modifications, bifurcations (or phase transitions) in other physical systems described by two variables with clearly separate time constants should show similar characteristics.

VI. FURTHER COMMENTS

Inspection of Figs. 2–4 shows that the average delay times match reasonably well the experimentally observed

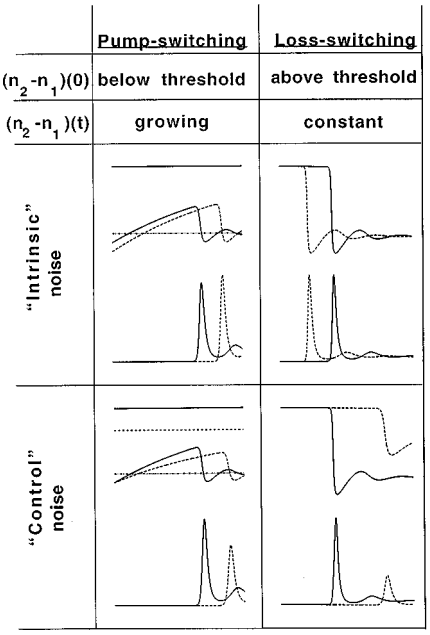

FIG. 11. Summary of the features of the distribution of the laser intensity peaks for the two different kinds of noise and types of turn-on. The line $(n_2-n_1)(0)$ represents the initial value of the population inversion; the line $(n_2-n_1)(t)$ represents its time evolution while the laser's field intensity is negligibly small. The top two figures illustrate the behavior of the population inversion (top lines in each rectangle) and of the laser intensity in response to a simulated intrinsic noise for the two different kinds of switch-on (in the case of loss switching we have chosen different initial conditions for the field intensity). The curves in the bottom boxes illustrate the response of the laser to control noise.

ones (cf. Fig. 5) [19]. The small time spreads that we observe in the distribution of points obtained numerically have to be attributed to the small amount of noise that we use for the simulations (a point already discussed) and to the fact that in the numerical simulation we add noise only to the initial condition and not to the whole trajectory. Hence we can consider the reproduction of the temporal behavior of the laser obtained from this model [3,6] quite satisfactory. On the other hand, such agreement cannot be found for the peak amplitudes if we compare the results of our simulations (Figs. 6, 8, and 10) to the experimental measurements (cf. Ref. [2]). This is a well-known weakness of CO_2 laser models, but does not reflect negatively on the qualitative description of the phenomena in which we are interested. However, no quantitative conclusions can evidently be drawn from the comparison between experiment and simulations.

VII. CONCLUSION

With the help of the numerical integration of a well-accepted model that describes the behavior of a CO_2 laser in the presence of different kinds of noise, we have confirmed the heuristic intepretation of the transient statistics for pump and loss switching proposed in Ref. [2]. The predominance of intrinsic over control noise highlights the dynamical behavior of the population inversion and the role of its initial condition in pump switching.

We have further identified the role that each of the differ-

ent noise sources plays in the turn-on of a class-*B* laser and determined the effect of the superposition of different noise sources (in different strengths). A graphical representation of the details of the dynamical evolution of the laser's variables has allowed us to illustrate clearly the physical processes behind the various slopes in the statistical distribution of peak amplitudes versus delay times for both pump and loss switching.

ACKNOWLEDGMENTS

L.M.H. and G.L.L. are grateful to H. Grassi, C. Green, and J. R. Tredicce for discussions in conjunction with the experimental work. Travel funding was provided by the French and Italian governments through the joint exchange program Galilée.

APPENDIX A

The expressions for the steady states (indicated with the overbar) that were used as initial conditions (independent of the normalization of time and of the relaxation rates) are

$$\overline{n_2}=\left\{\left(z\gamma_R+\gamma_1-\frac{z\gamma_R}{\gamma_R+\gamma_1}\right)+\gamma_2\left(1+\frac{z\gamma_R}{\gamma_R+\gamma_2}\right)P'\right\}\times\left\{2z\gamma_R+\gamma_1+\gamma_2-z\gamma_R^2\left(\frac{1}{\gamma_R+\gamma_1}+\frac{1}{\gamma_R+\gamma_2}\right)\right\}^{-1}, \tag{A1a}$$

$$\overline{n_1}=\overline{n_2}-1, \tag{A1b}$$

$$\overline{i}=\left(z\gamma_R+\gamma_1-\frac{z\gamma_R^2}{\gamma_R+\gamma_1}\right)\overline{n_1}, \tag{A1c}$$

$$\overline{m_1}=\frac{z\gamma_R}{\gamma_R+\gamma_1}\,\overline{n_1}, \tag{A1d}$$

$$\overline{m_2}=\frac{z\gamma_R}{\gamma_R+\gamma_2}\,\overline{n_1}+\frac{z\gamma_2}{\gamma_R+\gamma_2}P'. \tag{A1e}$$

The program calculates the initial values on the basis of the control parameter, then adds a very small $[O(10^{-20})]$ constant to the intensity i (to allow the code to move away from the unstable fixed point), and integrates the equations with the control parameter already above threshold. Noise is added to the desired variable (or parameter) after calculation of the steady state. The values of the model parameters, kept constant throughout all simulations (unless otherwise specified), are

$$K=2\times10^7\ \mathrm{s}^{-1}, \tag{A2a}$$

$$\gamma_R=7\times10^5\ \mathrm{s}^{-1}, \tag{A2b}$$

$$\gamma_1=8\times10^4\ \mathrm{s}^{-1}, \tag{A2c}$$

$$\gamma_2=1\times10^4\ \mathrm{s}^{-1}, \tag{A2d}$$

$$z=16. \tag{A2e}$$

APPENDIX B

For the integration of the model in the case of loss switching we use the equations in a slightly different form, which gives direct access to the control parameter. Equations (1) take the forms

$$\frac{ds}{d\tau}=K_{\mathrm{th}}[(n_2-n_1)-k], \tag{B1a}$$

$$\frac{dn_1}{d\tau}=-(z\Gamma_R+\Gamma_1)+\alpha(n_2-n_1)e^s+\Gamma_R m_1, \tag{B1b}$$

$$\frac{dn_2}{d\tau}=-(z\Gamma_R+\Gamma_2)-\alpha(n_2-n_1)e^s+\Gamma_R m_2+\Gamma_2, \tag{B1c}$$

$$\frac{dm_1}{d\tau}=-(\Gamma_R+\Gamma_1)m_1+z\Gamma_R n_1, \tag{B1d}$$

$$\frac{dm_2}{d\tau}=-(\Gamma_R+\Gamma_2)m_2+z\Gamma_R n_2+z\Gamma_2, \tag{B1e}$$

where

$$\alpha=(\sqrt{\gamma_R K_{\mathrm{th}}})^{-1}, \tag{B2a}$$

$$s=\ln i, \tag{B2b}$$

$$K_{\mathrm{th}}=\alpha K_{\mathrm{th}}, \tag{B2c}$$

$$K(t)=K_{\mathrm{th}}k(t). \tag{B2d}$$

$K(t)$ represents the time-dependent losses and all the other constants Γ_j are normalized as in Eqs. (3), but with respect to the threshold losses K_{th}. The choice of the variable s logarithm of the intensity i is made to facilitate the numerical integration of these equations, which are somewhat harder to handle than those for pump switching. Notice that the pump value does not explicitly enter into the equations any longer since the lasing threshold is now determined by the loss level and the pump intervenes only in determining the amount of unsaturated population inversion (below threshold). The steady states for the variables, above threshold, are

$$\overline{n_1}=\overline{n_2}-k, \tag{B3a}$$

$$\overline{m_1}=\frac{z\Gamma_R}{\Gamma_R+\Gamma_1}\,\overline{n_1}, \tag{B3b}$$

$$\overline{m_2}=\frac{z\Gamma_R\overline{n_2}+z\Gamma_2}{\Gamma_R+\Gamma_2}, \tag{B3c}$$

$$\overline{n_2}=\frac{\Gamma_1\left(1+\frac{z\Gamma_R}{\Gamma_R+\Gamma_1}\right)k+\Gamma_2\left(1+\frac{z\Gamma_R}{\Gamma_R+\Gamma_2}\right)}{\Gamma_1\left(1+\frac{z\Gamma_R}{\Gamma_R+\Gamma_1}\right)+\Gamma_2\left(1+\frac{z\Gamma_R}{\Gamma_R+\Gamma_2}\right)}, \tag{B3d}$$

$$\overline{i}=\frac{-(z\Gamma_R+\Gamma_2)\overline{n_2}+\Gamma_R\overline{m_2}+\Gamma_2}{\alpha(\overline{n_2}-\overline{n_1})}. \tag{B3e}$$

Because of the normalization chosen here, the steady states above threshold depend on the amount of losses and in Fig. 10 the trajectories converge to different levels. Furthermore, given the fact that, in this form of the model, the pump strength fixes only the unsaturated level of population inversion, pump or population noise now play the same role and in the text have been collected into one noise source (population noise).

[1] S. Balle, M. San Miguel, N. B. Abraham, J. R. Tredicce, R. Alvarez, E. J. D'Angelo, and R. Roy, Phys. Rev. Lett. **72**, 3510 (1994).
[2] H. Grassi, C. Green, L. M. Hoffer, G. L. Lippi, and J. R. Tredicce, Phys. Rev. A **50**, 805 (1994).
[3] R. Meucci, M. Ciofini, and Peng-ye Wang, Opt. Commun. **91**, 444 (1992).
[4] A. Yariv, *Introduction to Optical Electronics*, 2nd ed. (Holt, Rinehard and Winston, New York, 1976).
[5] G. L. Oppo, L. M. Narducci, and J. R. Tredicce, Opt. Commun. **69**, 393 (1989).
[6] M. Ciofini, A. Politi, and R. Meucci, Phys. Rev. A **48**, 605 (1993).
[7] A. Arimondo, F. Casagrande, L. A. Lugiato, and P. Glorieux, Appl. Phys. B **30**, 57 (1983).
[8] J. Dupré, F. Meyer, and C. Meyer, Can. J. Phys. **54**, 205 (1975); Rev. Phys. Appl. **10**, 286 (1975).
[9] W. J. Witteman, *The CO_2 Laser*, edited by K. Shimoda, Springer Series in Optical Sciences Vol. 53 (Springer, Berlin, 1987).
[10] A. J. DeMaria, Proc. IEEE **61**, 731 (1973).
[11] F. T. Arecchi, W. Gadomski, R. Meucci, and J. A. Roversi, Phys. Rev. A **39**, 4004 (1989).
[12] G. Marsaglia and A. Zaman, Florida State University Report No. FSU-SCRI-87-50, 1987 (unpublished), routine modified by F. James.
[13] W. H. Press *et al.*, *Numerical Recipes in C* (Cambridge University Press, Cambridge, 1990), p. 217.
[14] The amount of noise chosen for the integration must be small if one wants to obtain linear dependences in the distributions of the peak amplitudes as a function of delay time. This is due to the fact that the predictions of Ref. [1] are based on the assumption that the linear term in the Taylor expansion of the intensity suffices to describe the system's behavior [cf. Eq. (6) in that paper] and hence the numerical values for the noise have to be chosen to be correspondingly small.
[15] The clustering of points at given time intervals is due to the time resolution chosen for the output of points and is therefore a numerical artifact. Likewise, the small scatter in the peak intensity, observable in this (and other) figure(s), is due to the fact that points corresponding to different intensities have been forced to the same discretized time value.
[16] The presence of noise in two parameters widens considerably the time interval over which the peak in the laser intensity appears. Hence the artificial clustering of the points, observed in Fig. 2, does not appear.
[17] P. Spano, A. Mecozzi, and A. Sapia, Phys. Rev. Lett. **64**, 3003 (1990).
[18] S. Balle, P. Colet, and M. San Miguel, Phys. Rev. A **43**, 498 (1991).
[19] One must remember that, due to its particular excitation mechanism, the CO_2 laser has an intrinsic delay between the application of the turn-on pulse (for pump switching) and its actual effect on the upper level of the transition, which is of the order of 10^{-4} s [9]. This additional delay, mainly due to the collision dynamics in the discharge, is not reproduced by the model and hence the numerically simulated delay times are always shorter.